



## CFD SIMULATION OF LONGITUDINAL VENTILATION SYSTEMS IN A SCALED SHORT TUNNEL

Salih KARAASLAN, Ender HEPKAYA and Nuri YUCEL

Gazi University, Faculty of Engineering, Department of Mechanical Engineering, 06570 Maltepe-Ankara, TURKEY  
[karaaslansalih@gazi.edu.tr](mailto:karaaslansalih@gazi.edu.tr), [enderhepkaya@gazi.edu.tr](mailto:enderhepkaya@gazi.edu.tr), [nuyucel@gazi.edu.tr](mailto:nuyucel@gazi.edu.tr)

(Geliş Tarihi: 15. 07. 2011, Kabul Tarihi: 07. 10. 2011)

**Abstract:** In this study, a horseshoe cross-sectioned, short tunnel was considered. To simulate fire scenarios, a rectangular fire pool was placed in centreline of the tunnel floor. At different cross-sections of the tunnel, jet fan groups were installed and each fan group includes three jet fans. In order to simulate the fire induced smoke, the species transport model was used. Fires with 10 and 50 MW were considered for the simulations. The effects of LVS (Longitudinal Ventilation System) on the smoke movement and temperature distribution were numerically investigated by using the commercial CFD code FLUENT. Especially, simulations were conducted for the worst scenarios. After the fire induced smoke filled a big part of the tunnel, in order to determine the optimal ventilation approaches, combination of different fan groups were operated with various pressure jumps. From the simulations, it was observed that the smoke propagation was faster than the long tunnel studies found in the literature. It was also observed that the smoke velocity increases toward the tunnel entrance in the backlayer. In order to prevent this uncontrolled smoke movement, the best charge velocities and operation order of jet fan groups were determined numerically. It was observed that the operation order of fan groups, pressure jump values of fans and start time of the fans are important parameters to extinguish.

**Keywords:** Tunnel fires, Longitudinal ventilation, CFD, Smoke extraction .

## ÖLÇEKLENDİRİLMİŞ BİR TÜNELDE EKSENEL HAVALANDIRMA SİSTEMİNİN CFD SİMÜLASYONU

**Özet:** Bu çalışmada at nalı kesitli, kısa bir tünel incelenmiştir. Yangın kaynağını simüle etmek için tünel zemininin merkezine dikdörtgenler prizması şeklinde bir yangın havuzu yerleştirilmiştir. Her biri üçer adet fan içeren, jet fan grupları tünelin farklı kesitlerine yerleştirilmiştir. Yangın kaynaklı duman, türlerin taşınımı (Species Transport) modeli kullanılarak simüle edilmiştir. Bu çalışmada, eksenel havalandırma sisteminin yangın kaynaklı duman hareketine ve sıcaklık dağılımına etkisi FLUENT yazılımı kullanılarak nümerik olarak incelenmiştir. Çalışmada, yangın kaynaklı dumanın tünelin büyük bir bölümünü kaplaması beklenmiş, tahliye için kullanılacak olan optimum havalandırma yaklaşımının elde edilmesi için fan grupları farklı sıra ve itiş güçleri için değerlendirilmiştir. Simülasyon sonunda, duman yayılımının literatürde yer alan uzun tünellere oranla daha hızlı olduğu görülmüştür. Ayrıca tünel girişine yaklaştıkça, tavan bölgesinde meydana gelen geriye akış hızının arttığı hesaplanmıştır. Bu kontrolsüz duman yayılımının önlenmesi için en iyi havalandırma hızı ve jet fan operasyon sırası nümerik olarak belirlenmeye çalışılmıştır. Çalışmanın sonunda fan gruplarının çalışma sırası, itiş güçleri ve havalandırmaya başlama zamanlarının bu tip yangınlar üzerinde önemli bir parametre olduğu kanaatine varılmıştır.

**Anahtar Kelimeler:** Tünel yangınları, Eksenel havalandırma, CFD, Duman tahliyesi.

### NOMENCLATURE

$A_C$	Cross-sectional area [m <sup>2</sup> ]
$C_p$	Mixture specific heat [kJ/kgK]
$D_h$	Hydraulic diameter [m]
Fr	Froude number
g	Gravitational acceleration [m/s <sup>2</sup> ]
k	Turbulent kinetic energy [m <sup>2</sup> /s <sup>2</sup> ]
L	Characteristic length [m]
$\dot{m}_{air}$	Air mass flow rate [m <sup>3</sup> /s]
$\dot{m}_{CO_2}$	Carbon dioxide mass flow rate [m <sup>3</sup> /s]
$\dot{m}_{gas}$	Gas mass flow rate [m <sup>3</sup> /s]

q	Heat release rate [MW]
$q_s$	Scaled heat release rate [MW]
Re	Reynolds number
T	Ambient temperature [K]
$T_f$	Temperature of fire ambient [K]
$T_{gas}$	Temperature of the combustion gases [K]
U	Velocity [m/s]
$U_s$	Scaled velocity [m/s]
$V_C$	Critical velocity [m/s]

### Greek Symbols

$\varepsilon$	Dissipation rate of turbulent kinetic energy [m <sup>2</sup> /s <sup>3</sup> ]
$\rho$	Density [kg/m <sup>3</sup> ]

$\emptyset$	Scale factor
$\omega$	Specific dissipation rate of turbulent kinetic energy

### Acronyms

CFD	Computational Fluid Dynamics
FG	Fan Group
HRR	Heat Release Rate
JF	Jet Fan
LVS	Longitudinal Ventilation System
PIARC	Permanent International Association of Road Congress
SST	Shear Stress Transport

## INTRODUCTION

In the last century, there were dozens of catastrophic fires in underground transportation systems, like Saint Gotthard tunnel in Switzerland in 2001, Tauern tunnel in Austria in 1999 and King's Cross in London in 1987. The King's Cross subway station fire is supplying very important information about fire fighting. The ditch effect which is the one of prominent effect on fire was discovered after analyzing this fire. Another very important fire event in history is Daegu subway station fire (South Korea in 2003) which proved there is no way to be ready for a catastrophic fire even in the most modern subway stations. In this event 198 people lost their lives and hundreds of them were wounded by the smoke. Another noticeable fire event was English Channel tunnel, which caused high cost damage in the structure, in 1996. Due to the fire events in the history, researchers have worked on the subjects of fire experimentation, smoke discharging and tunnel ventilation systems.

In literature, there are many comprehensive studies on fire researches that have been performed by using experimental, numerical and analytical methods. But, generally, only experimental and numerical studies or both experimental and numerical studies with full-scale or reduced scale tunnel models are preferred to predict the fire and ventilation scenarios.

Hu et al.(2010) analyzed and compared longitudinal decay profiles of CO concentration and smoke temperature in a tunnel fire smoke flow theoretically. Experimental data on longitudinal CO distribution achieved from a set of full scale road tunnel fire tests were presented to compare with the theoretical equation. CFD simulations were also carried out by Fire Dynamics Simulator (FDS). The full scale experimental data and the CFD simulation results both agree well with the theoretical analysis and equations. Hu et al. (2008) studied the back-layering length and critical longitudinal ventilation velocity in tunnel fires. A semi-empirical model was formulated and compared with former expressions in literature. An equation to predict the critical longitudinal ventilation velocity was further derived by setting the back-layering length to be zero. The results from the full-scale burning tests were applied to examine this equation. In addition, some

scenarios were simulated using a CFD code. The critical velocities predicted were similar to those observed in the field tests, CFD simulations and estimation by a simple model by Thomas. As the plume configuration, for a bigger tunnel fire was not the same as that for a small fire, other empirical expressions for large tunnel fires gave some lower critical velocity in comparison with the result for small tunnel fire. Kurioka et al. (2003) conducted experiments using three kinds of tunnel model to understand fire phenomena in the near field of a fire source. Square fire sources were employed as model fire sources. The aspect ratio of the tunnel cross-section, heat release rate and longitudinal forced ventilation velocity were varied. Empirical formulae for flame tilt, apparent flame height, maximum temperature of the smoke layer and its position were developed based on the results obtained in the 1/10 scale model tunnel. It was also confirmed that these empirical formulae were sufficiently applicable for predicting fire phenomena in the near field of square fire source from the comparison with the results in 1/2 and full scale experiments.

Hu et al. (2007) conducted tests to study the distribution of smoke temperature along the tunnel ceiling in the one-dimensional spreading phase. The fire size and the height above the floor, the tunnel section geometry and longitudinal ventilation velocity varied in these tests. Experimental results showed that when the fire size was larger, the smoke temperature below the ceiling was higher, but it decayed faster while travelling down the tunnel. The longitudinal ventilation velocity seemed to take much influence on the smoke temperature decay speed downstream. A "barrier effect" was shown for the smoke temperature distribution of the upstream back layering. Results showed that model over estimated the decay speed of ceiling jet temperature for the downstream flow. However, good agreement was achieved between the measured data and the model predictions for the upstream back layering.

A comprehensive full-scale numerical and experimental works were performed by Vega et al. (2008). In order to investigate various fire scenarios and ventilation approaches, Memorial Tunnel was rearranged. Also a model of Memorial Tunnel was used for CFD analysis with important modeling techniques. In that study, it was shown that CFD simulation results for LVS (Longitudinal Ventilation System) on fires are in agreement with experimental results hence these results can be used safely. Tajadura et al. (2006) modeled a tunnel which was a section of Inner Belt Roadway-Barcelona tunnel that has ascending and descending galleries. The slope of the tunnel, combined with its reduced height, caused a predominant propagation of the smoke in the ascending direction. Lee et al. (2006) carried out numerical simulations to analyze the effect of the aspect ratio on smoke movement in tunnel fires. The tunnel models were scaled by a factor of 1/20 for experiments and numerical analysis. Temperatures were in good agreement with experimental results. Aspect ratio of the tunnel cross-section affected the growth and

development of smoke in tunnel fires. It was confirmed that high-temperature smoke moves along the ceiling and cool air flows in along the lower part of the tunnel by the analysis of temperature and velocity contours. A different numerical study on tunnel fires was conducted by Modic (2003). The critical velocity formula and the fire site gas temperature were adapted from ASHRAE Applications (1999).

In these studies, the calculated smoke propagation velocity/time and required time for people's escape were discussed. Hwang et al. (2005) used CFD code to model floor-level fires in a ventilated tunnel. The computer code was verified by checking the computed velocity profile against experimental measurements. The CFD results showed the leveling-off of the critical ventilation velocity as the heat release rate surpasses a certain value. At this critical ventilation, the ceiling temperature above the fire reaches a maximum. The CFD results are compared with two simple theories of critical ventilation by Kennedy et al. (ASHRAE Trans. Res. 102(2) (1996) 40) and Kunsch. Jojo et al. (2003) presented CFD simulations on a full scale tunnel with different fire scenarios. The parameters varied were the fire size, ventilation system and its capacity. Furthermore, sensitivity analysis on the effects of the grid size, and number of iterations on the required computing time and accuracy of the results were carried out.

Another important issue is critical ventilation velocity determination and pretty many studies focused on this term. Vauquelin et al. (2006) investigated the effect of tunnel width on the critical velocity. He showed that there is a relation between tunnel width and critical velocity based on experimental, numerical and also analytical studies. These studies were performed on a scaled tunnel model by applying scaling rules. Hu et al.(2008) compared five different empirical critical velocity formula results, CFD results and the experimental results according to the location of the fire. The validity of CFD result was discussed and it was shown that it is in good agreement with experimental results.

Wu and Bakar (2000) carried out a series of experimental tests to determine the critical ventilation velocity in five scaled tunnel models having the same height but different cross-sectional geometries. The tunnel hydraulic diameter was used as the characteristic length. Depending on the fire heat release rate, two different critical ventilation velocity variation regimes were observed. At low rates of heat release, non dimensional critical ventilation velocity varies as one-third power of the non-dimensional heat release rate. However, at higher heat release rates, non-dimensional critical ventilation velocity becomes independent of the fire heat release rate. Also in this study comprehensive CFD simulations were carried out to examine the flow behavior inside some of these scaled tunnel models. In order to obtain required ventilation velocities, modeling axial jet fans have importance for LVS. For instance, Betta et al. (2009 and 2010) used a momentum source technique. It was useful for getting desired jet fan

discharge velocities instead of modeling complex solutions and geometries in these studies.

In the literature, there have been a number of studies related to smoke control and longitudinal ventilation of road tunnel. However, only a few of works were focused on the smoke control of a short road tunnel. The tunnels can be defined as "short" up to 800 m according to many roadway criterion. Turkey is the country which has plenty of short road tunnels. In short tunnels, the smoke propagation will spread faster and so, design and optimization of the ventilation system for smoke evacuation has importance on this subject. In this case study, numerical approximation was conducted to investigate the optimal longitudinal ventilation approach and extraction of fire induced smoke strategies for a designed fire scenario in the horseshoe cross-sectioned Asarkayası short road tunnel in Ordu/Turkey.

The transient smoke spread velocity and temperature distributions in the tunnel were simulated using a commercial software package, FLUENT v6.3.26 to solve the three dimensional Navier-Stokes equations for flow analysis, energy conservation equations and smoke particulate transport equations on a considered domain. In order to develop the optimal smoke extraction strategy by using longitudinal ventilation system, the worst fire scenario was considered in the short tunnel. So, in this case study, mainly three important variables were discussed. These were critical velocity, smoke spreading volume in the tunnel and safe evacuation time.

## METHODOLOGY

### Tunnel Geometry and Model Description

In this study, a horseshoe cross-sectioned short tunnel *Asarkayası* was considered. The cross-sectional geometry and the dimensions of the tunnel are shown in Fig. 1. The length of the tunnel was taken as 300 m. The chosen tunnel model has two traffic lanes and two safety walk ways. Based on the dimensions given in Fig. 1, the cross-sectional area and the hydraulic diameter of the tunnel were calculated as  $72 m^2$  and 8.89 m, respectively.

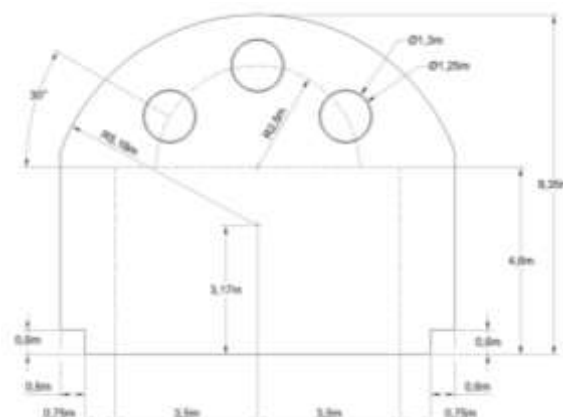


**Figure 1.** Dimensions of horseshoe cross-sectioned short tunnel.

For the longitudinal ventilation system, vane axial fans were used. The inner diameter of these fans is 1.25 m and each of them could deliver maximum  $86.9 \text{ m}^3/\text{s}$  (supply air up to  $\sim 73 \text{ m/s}$ ) of air. Each group of fans located at a cross-section consist of three fans. Fan groups are placed to the tunnel ceiling with 80 m distance from the entering portal and from each other. Location of the fan groups and fire pool are shown in Fig. 2.

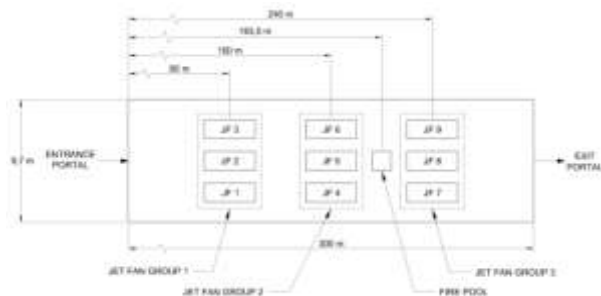


**Figure 2.** Location of the fan groups and fire pool.

In fire scenarios, the fire site is located at 183.5 m which is between fan group 2 and fan group 3. The fire pool considered has dimensions of 1.54 m x 2.3 m x 7 m (width x height x length). Since full scale simulations require high number of mesh points and hence long CPU time, a scaled version of tunnel was used in the numerical simulations. The similarity rules were applied to scale the model. In order to get useful results in experimental or numerical simulations in the scaled model, there must be a well defined similarity between the scaled model and prototype. If there is a strong similarity, a scaled model can be used to investigate specific aspects of the behaviour of the fire or smoke. If the similarity is not so strong, the behaviour of the fire can only provide information in general terms. In order to define similarity between prototype and scaled model, it is necessary to consider mass balance and the gas flow at faces of the fire pool on the scaled model. We used Froude number to characterise fire and flow conditions in the scaled tunnel.

$$Fr = \frac{U^2}{gL} = \frac{\text{inertial forces}}{\text{bouyancy forces}} \quad (1)$$

Other non-dimensional numbers are also used to classify flow behaviour, including the Reynolds number, the Richardson number and the Grashof number which is essentially a combination of the Reynolds and Richardson numbers. Ideally each of these numbers should be the same in the scaled model and in prototype. In reality however, this is not possible and models are usually scaled considering the equality of the Froude numbers only. As pointed out by Carvel (2009), if the scaling factor is not very high the equality of Froude number on model and prototype tunnels is a reasonable approach to define similarity of tunnel fire. Otherwise the equality of Reynolds number must also be considered. In the present study, the scale factor is chosen as 1/20 therefore equality of Froude number is considered to be adequate for the similarity. Using similarity of Froude Numbers in the model and

prototype, the relations between velocity, heat release rate and scale factor  $\emptyset$  can be obtained. Assuming the scaling factor is known, velocity and heat release rate in the model tunnel can be calculated by using the following equations.

$$U_s = \sqrt{\emptyset} U \quad (2)$$

$$q_s = \sqrt{\emptyset^5} q \quad (3)$$

## Mesh Construction

The mesh was created in ANSYS Gambit v2.4 software. In constructing the mesh, the supports used to mount the jet fans to the ceiling were ignored, considering that their effect on the flow would be negligible. Similarly, the casing of the jet fans was ignored because of the same reason. The jet fan blades, rotors etc. also were not included in the model, since the aim of this study was not to investigate the fan performance or flow characteristics of fans. To represent the fans in the flow field, a sub domain whose cross sectional area is the same as the fan outlet area was specified along the tunnel. To locate the fan inlet and outlet, this specified sub domain was sliced along the tunnel.

Different mesh elements with the same element numbers were used to determine suitability of the mesh elements for our geometry. As a result, the Hex/Wedge element with the type of Cooper was found to be suitable. Refined meshes were introduced to the different zones of computational domain where required: Over the fire site to take care of the high gradients of the variables; in the jet fan inlets-outlets to improve the accuracy of momentum transfer and also at the tunnel inlet and outlet to improve the accuracy on representing the boundary conditions.

## Boundary Conditions

The boundary conditions were set as follows:

**1- ) Smoke source:** Due to short tunnel is considered in this study, smoke spreads to the portals very fast. Therefore, by a simplification, a constant heat release rate (HRR) approximation without any chemical reaction modelling was adopted and only heat convection was considered in the fire source. Generally, the heat release rates were proportional with the square of time and then remains constant at maximum value. But this approach causes fast propagation to the portals in short tunnels, the smoke goes out in seconds. On the other hand, these time dependent heat release rates reaches the constant section in a few minutes. So, in order to obtain optimum ventilation strategy for the worst cases, considering only the constant heat release rate section seemed an appropriate approach. In the numerical simulations, 10 MW and 50 MW fire situations were considered. These fire heat release rates represent the fires of an automobile and an oil tanker respectively. The mass fractions of combustion products were prescribed based on the data provided by

EUREKA-Project EU 499: Firetun, 1995. According to this data base, CO<sub>2</sub> and air mass fractions were taken as 95% and 5% for 10MW fire, and 91% and 9% for 50 MW fire, respectively. Beside the mass fractions, input temperatures for 10MW and 50 MW fire cases were taken as 573.15 K and 950 K, respectively (adapted from PIARC and Committee on Road Tunnels, 1999). Radiation was not modelled due to complexity of radiation modelling like as Vega, Wu and Bakar etc. According to the results presented by PIARC and Committee on Road Tunnels (1999), approximately 2/3 heat power of fires in road tunnel contributed to the heat convection, so heat release rate (HRR) was reduced by 35% in this study. This approximation gives compatible results with the experimental results including both radiation and convection heat transfer mechanisms. The same assumption was done by Vega et al. (2006) for Memorial Tunnel Test Cases.

**2- ) Initial Operating Condition:** The operating temperature and air density inside the tunnel were assumed at 300 K and 1.225 kg/ m<sup>3</sup>, respectively.

**3- ) Boundary conditions for Tunnel:** The surface roughness height of tunnel wall was set to 0.005 m, and the tunnel wall was considered to be adiabatic because of the location of tunnel under the mountains, the inlet and exit portals of tunnel were specified with “velocity inlet” and “pressure-outlet” respectively. The simulations were performed on a windy day at 1 m/s air inlet velocity to tunnel entrance.

**4- ) Axial Jet fans:** At the impeller and rotor part of jet fan, the module “Fan” in software FLUENT v6.3.26 was applied, and the pressure jump values were set for 27 Pa and 54 Pa for obtaining the discharge velocities of 30 m/s and 48 m/s (after scaling: 7 m/s and 9 m/s ) respectively. These velocity values were selected considering the critical velocity magnitudes.

### Solver Set and Simulation Approach

The velocity, smoke and temperature distributions in the tunnel were simulated using a commercial software package, FLUENT v6.3.26 which uses the finite volume method to solve three dimensional Navier-Stokes equations on an unstructured grid. The Realizable k- ε turbulence model was chosen after a comparative study between Realizable k- ε and k- ω-SST. This comparison showed that Realizable k- ε model converges faster and fluctuates less than SST k- ω model.

To obtain temperature distribution, energy equation was included in the model. The solver of FLUENT was Pressure-Based, unsteady and implicit solver. For the velocity-pressure coupling, SIMPLE algorithm was used. The second order upwind discretization was used for convective terms and a central difference scheme was used for diffusive terms. Gravitational body forces were included in the momentum equations introducing buoyancy terms by using Boussinesq approach. In calculations, the time step size was chosen as 0.05 s and

maximum iteration in each time step was chosen as 40. The time step size 0.05s was calculated by using Courant Number analogy. The average element size is about 1 cm and average flow velocity is about 0.22 m/s (scaled velocity value) so, in order to obtain the Courant Number smaller than 1, the time step size was found ~0.045-0.05s. Thus, the skipping the changes between the elements were prevented in the solution algorithm. The computations were carried out on a PC with 2.4 GHz and 2 GB RAM. For each case, computations took approximately 100 hours. Generally, most of fire simulations in the literature (Modic, 2003) were made without combustion models to avoid extreme complexity due to uncertainty of combustion models and the fuel load. In this study also, fire was modelled as a source of mass that represents smoke release over only upper surface of the rectangular fire pool in the tunnel. The mass balance was insured by air supplied from the back surface of the fire pool. Smoke release and air supply are schematically shown in Fig. 3. The mass flow rate of smoke released and mass flow rate of air supplied to the fire pool were calculated by using the formulas which were based on heat release rate (HRR) given by Vega et al. (2008):

$$\dot{m}_{gas} = \frac{W}{c_p(T_{gas}-T_0)} \quad \text{And} \quad \dot{m}_{air} = \dot{m}_{gas} - \frac{1}{3}\dot{m}_{CO_2} \quad (4)$$

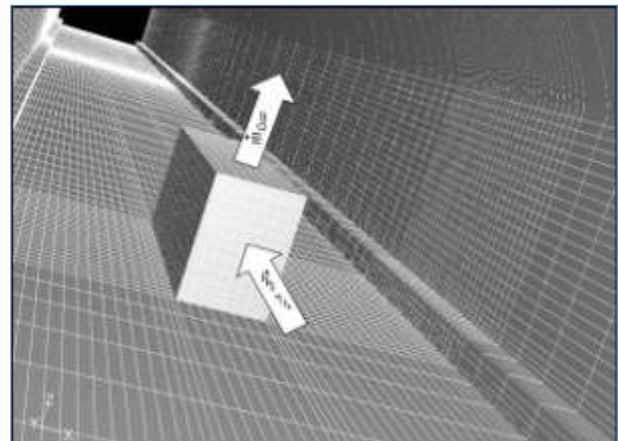


**Figure 3.** Mass balance of fire source

First, the flow characteristics in the tunnel were investigated numerically by using only air inlet velocity to tunnel entrance, while the fans were not operated. After the flow characteristics of air were obtained, the fire was started to investigate the smoke movement at the tunnel ceiling zone. When the smoke reached maximum backlayering length, the jet fans were started to operate. The characteristics of the fire for 1/20 scaled tunnel are given in Table.1.

The jet fan groups were operated from 1 to 3 in different combinations. In order to identify different cases considered with different heat release rate, working fan groups and pressure jump values, an eight digit coding system was used.

**Table 1.** Fire characteristics for 1/20 scaled tunnel

Tunnel and Fire Properties	
Tunnel Length	15 m
Cross-Section Area	0.18 m <sup>2</sup>
Hydraulic Diameter	0.4445 m
Reynolds Number	6729.9
Inlet Velocity	0.22 m/s
$\dot{m}_{gas}$ (10 MW)	0.01244 kg/s
$\dot{m}_{CO_2}$ (10 MW)	0.000622 kg/s
$\dot{m}_{air}$ (10 MW)	0.012233 kg/s
$\dot{m}_{gas}$ (50 MW)	0.0248 kg/s
$\dot{m}_{CO_2}$ (50 MW)	0.00223 kg/s
$\dot{m}_{air}$ (50 MW)	0.024056 kg/s
Critical Velocity (10 MW)	0.62 m/s
Critical Velocity (50 MW)	1.225 m/s

In this coding system, first two digits indicate heat release rate, following three digits represent working fan group, and remaining three digits represent pressure jump value in the jet fans. In the ventilation test coding, (1) represents the pressure jump amount of 27 Pa and (2) represent the pressure jump amount of 54 Pa pressure difference between fan inlet and outlet. Hence, 50FG2 (1) coding represents, 50 MW fire with fan group 2 was working with pressure jump of 27 Pa. The ventilation test coding used in this study is presented in Table 2.

**Table 2.** The Ventilation Test Coding

Ventilation Tests Coding	HRR (MW)	Working Jet Fan Groups	Pressure Jump (Pa)
10FG1(1)	10	1	(1)
10FG1(2)+10FG2(1)	10	1-2	(2)-(1)
50FG1(1)	50	1	(1)
50FG1(1)+50FG2(1)	50	1-2	(1)-(1)
50FG1(2)	50	1	(2)
50FG1(2)+50FG2(2)	50	1-2	(2)-(2)
50FG1(2)+50FG2(2)+50FG 3(2)	50	1-2-3	(2)-(2)-(2)
50FG1(2)+ 50FG 2(1)	50	1-2	(2)-(1)
50FG1(2)+50FG2(1)+50FG 3(2)	50	1-2-3	(2)-(1)-(2)

The critical velocity was calculated by Thomas’ formula for ventilation scenarios:

$$V_c = \left( \frac{gD_h Q}{\rho T C_p A_c} \right)^{1/3} \quad (5)$$

It is seen from both experimental and numerical studies in the literature that the critical velocity formula of Thomas is reliable for central fires. The fire in present study was considered as a central fire and hence, Thomas’ formula was used to calculate the critical velocity (Hu et al., 2008).

### Element Number Optimization

Cartesian coordinate grid system was assigned along the x, y and z (vertical) directions. The tunnel was divided into nine portions along to the axial tunnel direction to simplify the meshing operation. Different grid systems were tested in *steady-state* simulations to decide optimal mesh density. For constant heat release rate of 10 MW fire case which was considered most severe case. The axial velocities at reference line which was located 7.5 m from inlet portal at the centre of the tunnel were drawn in Fig.4 for different size of meshes. As seen in this figure, by increasing mesh sizes, velocity profiles get closer to each other.

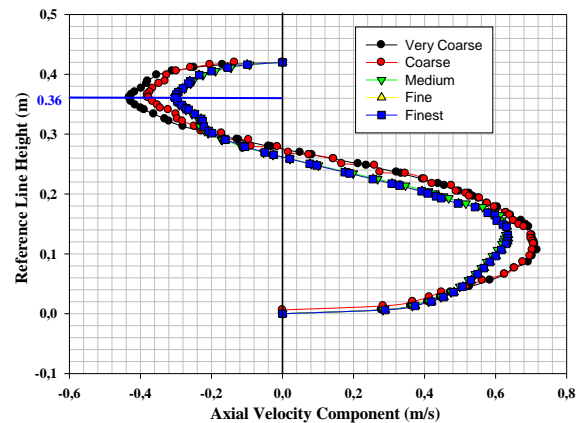


**Figure4.** Grid variation on backflow velocity on reference line at the centre of the tunnel.

The maximum backflow velocity occurs at the point of 0.36 tunnel height for all meshes considered. The backflow velocity values and deviation of backflow velocity with respect to finest mesh are given in Table.3.

As expected from these results, the computed solutions show larger deviations for the coarse meshes 1 and 2 while convergence is obtained for finer meshes 3, 4 and 5. Based on the results, grid independence is reached in mesh 3 and therefore, the following simulations have been conducted using this grid. Although both of the medium and fine meshes are under 1% deviation from the finest mesh, medium mesh was chosen to reduce the computation time. The total number of elements for the 15 m scaled short tunnel was chosen 505 292. Grid distribution of the model is shown in Fig. 5.

**Table.3** Grid Independence Study

<i>Mesh Fineness</i>	<i>Total Number of Elements</i>	<i>Computed Velocity at reference line (m/s)</i>	<i>Deviation From Finest Mesh (%)</i>
Mesh.1- Very Coarse	190 128	-0,4403	% 31
Mesh.2- Coarse	262 378	-0,3798	% 20.1
Mesh.3- Medium	505 292	-0,3055	% 0.62
Mesh.4- Fine	832 464	-0,3045	% 0.29
Mesh.5- Finest	1 165 448	-0,3036	-

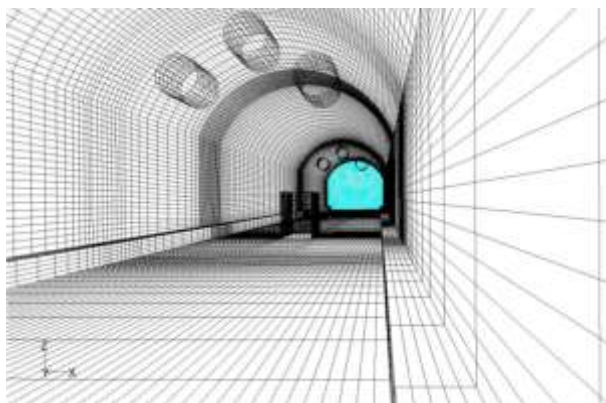


**Figure 5.** Grid definition of the model

## Results and Discussions

High temperatures can be extremely dangerous for people who were involved in a fire incident inside a road tunnel. The longitudinal ventilation system, LVS supplies cold fresh-air and this cold fresh air also contribute to reduce the temperature inside the tunnel. The system must keep a bearable temperature for the people in the affected zone; hence, the temporal changes in the temperature distribution inside the tunnel are extremely useful to observe the benefits of the LVS. It was considered that 50 MW fire case poses step changes in the variables. For this case, as convergence criteria, the residuals for the velocity components were set to  $10^{-6}$ , for turbulence parameters were set to  $10^{-5}$  and for combustion species were set to  $10^{-4}$  in all calculations. The residual data before and after ventilation for 50 MW fire case is shown in Fig.6. When ventilation starts, a jump in the residuals can be seen in this figure. This jump varies between  $10^{-2}$  and  $10^{-1}$ . The temperature distribution just before the ventilation system turned on for 10 MW and 50 MW fire cases are shown in Fig. 7.

To find an optimal ventilation scenario, the LVS simulations that are shown in the Table.2 were carried out.

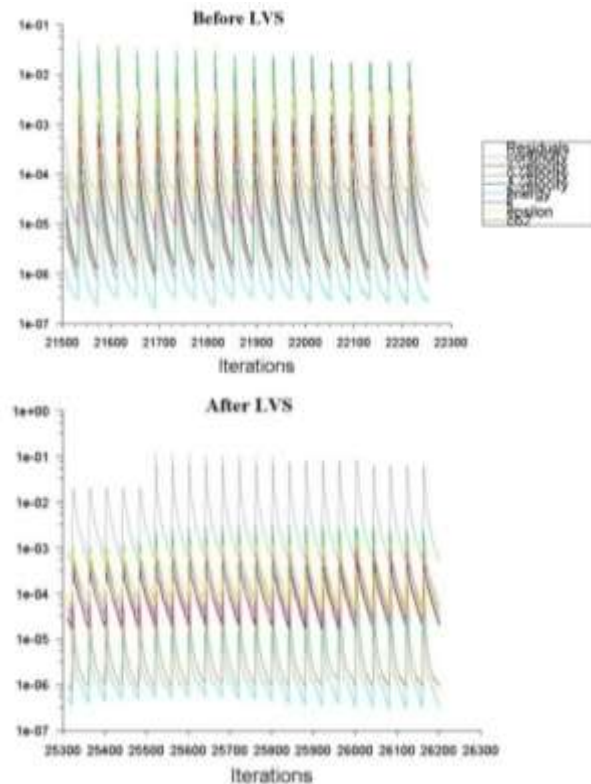


**Figure 6.** Residuals data of 50 MW fire case before and after LVS.

The goal of the ventilation was to clean the region between fan groups firstly, then exhaust the smoke to the outside. The jet fans were started at the time that the smoke reached the fan group 1. The simulations revealed that the time required for the smoke to reach the fan group 1 is 20 s and 10 s for 10 MW and 50 MW fire cases, respectively.

When the numerical simulations are evaluated together, it is observed that the cases 10FG1 (2) +10FG2 (1) and 50FG1 (2) result most suitable conditions to extract the smoke and to decrease the temperature inside the tunnel.

In a short tunnel considered, the smoke propagation to the portals is rather fast due to high velocities of hot fire gases. These gases in huge fires rise to the tunnel ceiling and cause high temperatures especially at the flame region (above the fire pool).

This smoke movement depends on time as shown in Fig. 7 above. The smoke travelled approximately 180 m in 30 s for both fire scenarios.

A comparison on smoke distributions of 10 MW and 50 MW fires over the fire pool cross-section is shown in Fig. 8. As seen in these figures, the transition temperatures from hot region to cold region are 313 K and 333 K for 10 MW and 50 MW cases, respectively.

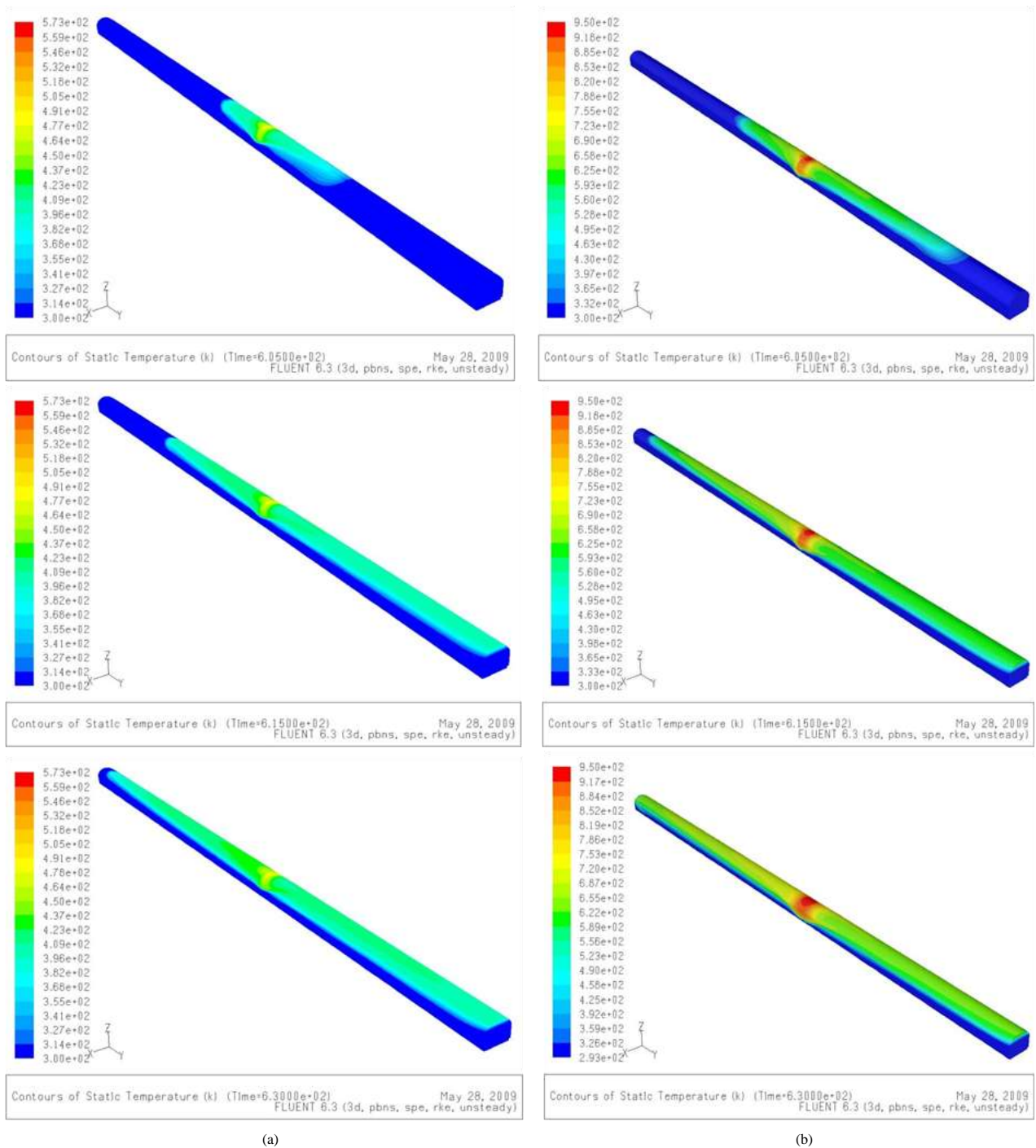


**Figure 7.** The smoke temperature distribution before the ventilation system is turned on: a) For 10 MW fire case at 5s, 15s and 30s b) For 50 MW fire case at 5s, 15s and 30s respectively (units in K).

The cross-section view of the temperature distribution shows the flame regions and the intensity difference between the fires. The hot fire gases moves to the tunnel ceiling due to the buoyancy effect and then turns back tunnel floor near the side walls. In 50 MW fire, this movement occurs faster than 10 MW fire case and hence the smoke reaches the floor (safety walkways) in a short time period. This situation can affect the human health and cause more serious problems.

For 10FG1 (2) +10FG2 (1) and 50FG1(2) simulations, the temperature distribution at the longitudinal vertical

centre plane of the fire zone just before and after the ventilation system is turned on are shown in Fig.9. For 10 MW fire case, the shape of the flame is clearly visible. After a smoke free region is attained between the jet fans, the flames tilt towards to exit direction. The effect of the LVS decreases the temperature and then the flames die in a short time. At case 50FG1(2), the space between the fans is also cleaned well.

However, the change on flame shape is very small compared to 10 MW fire case for same time period even though ventilation system is on. This is due to the high



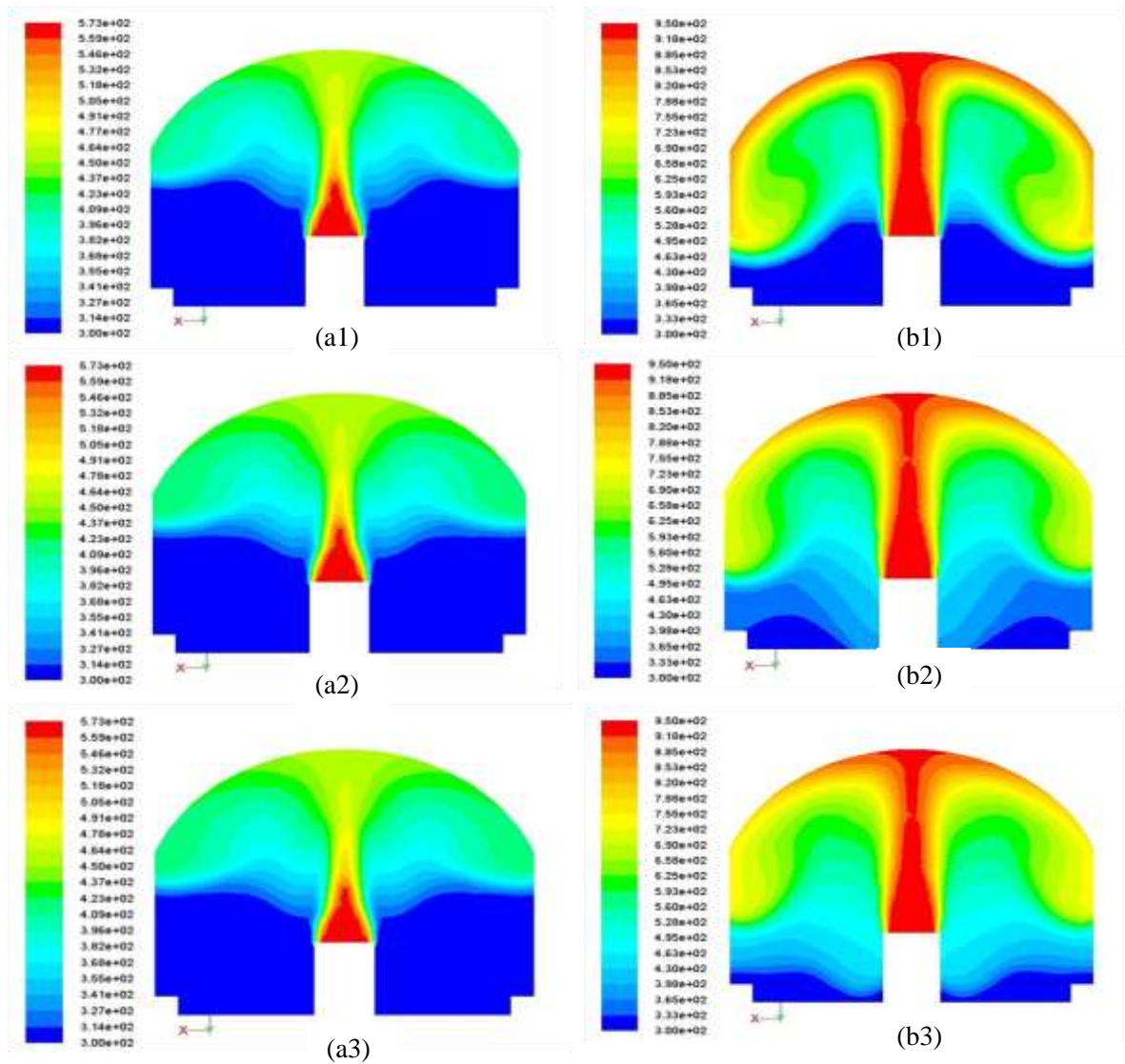


**Figure 8.** Fire Pool Cross-section smoke distribution before the ventilation system is turned on: (a) For 10 MW fire case at 5s, 15s and 30s and (b) For 50 MW fire case at 5s, 15s and 30s (units in K).

intensity of the 50 MW fire which requires more time to tilt down and to die. To prevent the dispersion of the hot gases around the fire pool, the jet fan group 2 were not operated. This operation type can result smoke in free region around the fire pool and to help fighting the fire.

The axial velocity profiles on the vertical centreline of cross – section at 6 m (120 m full scale tunnel) from the tunnel entrance which is located between fan groups 1 and 2 for 10 MW and 50 MW fires are shown in Fig. 10.

These curves represent the variation of velocities of the backlayering gases and ventilation air with time. As seen in these figures, before the ventilation began, there was a backlayering to the tunnel entrance in both fire cases, but the ventilation air which was charged above the calculated critical velocity pushes the smoke toward the tunnel exit gradually, and 15 s later from start of the ventilation, backlayering is got under control, velocity profiles remained in desired shape and the smoke-air mixture in the tunnel ceiling zone moves faster. Since the critical velocity value depends on HRR,

backlayering velocity for the 50 MW fire case is higher than 10 MW fire case, without operation of fans. After the ventilation fans are operated, due to the suction of the fans, negative velocities occur at the bottom part of the tunnel. The axial velocity profiles on the vertical centreline at a section located 2 m and 6.8 m from the tunnel entrance were also plotted before and after LVS for 10 MW (10FG1(2)+10FG2(1)) and 50 MW (50FG1(2)) in Fig. 11, Figure 12 and Fig 13. In 10 MW fire case, before the ventilation started, backlayering velocity exists at the selected vertical centrelines. Behaviour of velocity profiles is similar before LVS for 10 MW fire case. As seen Fig. 11 and Fig. 12 , velocity magnitude of ceiling zone at  $y=2\text{m}$  was bigger than at  $y=6.8\text{m}$  before ventilation. For the 10 MW fire, at the positions  $y=2\text{ m}$  and  $y=6.8\text{ m}$  the backflow velocities are approximately 0.58 m/s and 0.43 m/s respectively. This backlayer velocity difference at two different cross sections maybe attributed to the higher temperature difference at the cross section closer to the tunnel entrance. After LVS started, the behaviour of velocity

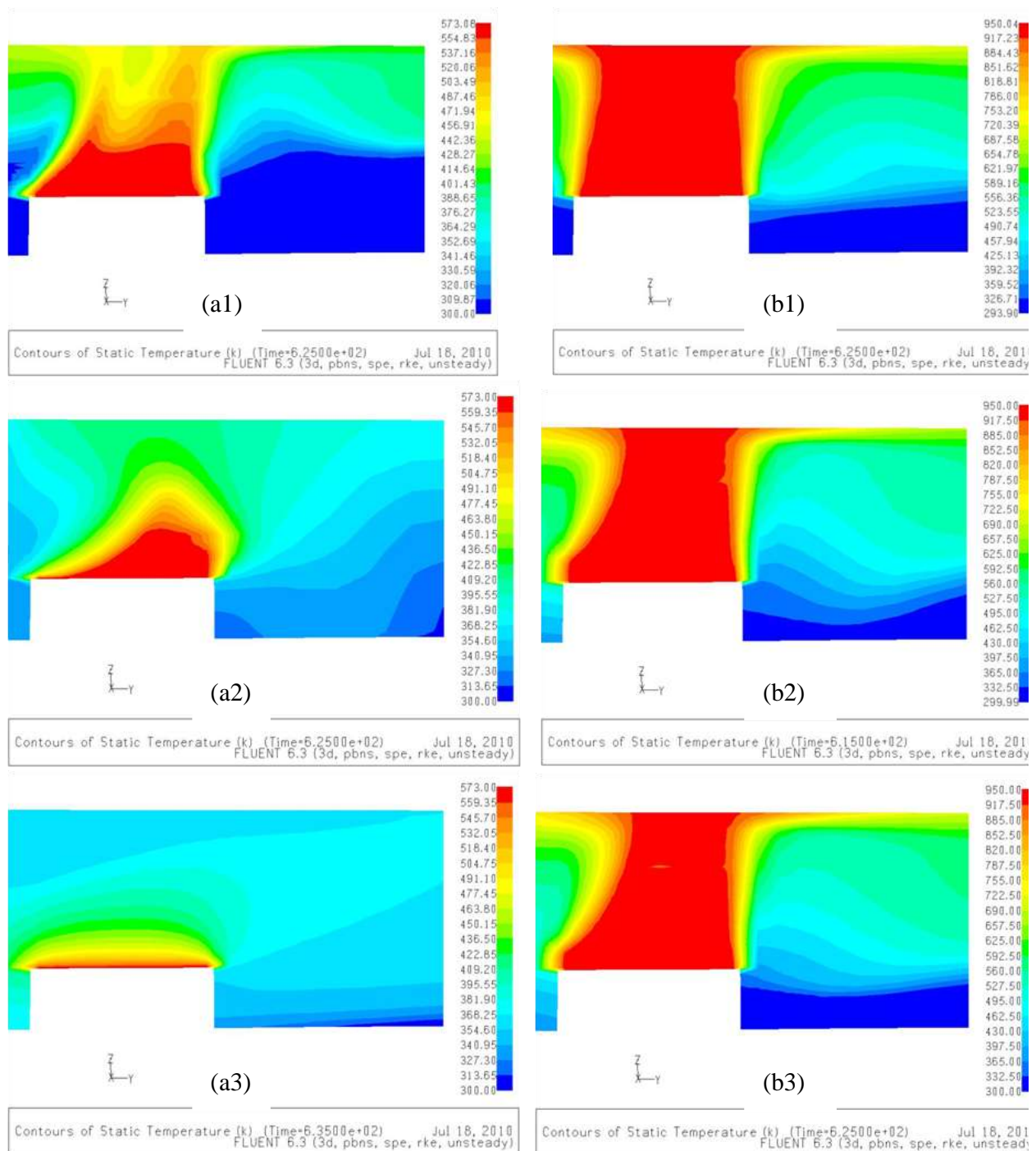


**Figure 9.** Temperature distribution at the centre plane of the fire zone just before and after the ventilation system is turned on: (a) For 10 MW fire case at 5s, 15s and 30s and (b) For 50 MW fire case at 5s, 15s and 30s. (test code representation 10FG1 (2) +10FG2 (1)) and (50FG1 (2))) (units in K).

profiles change dramatically. 15 s later from the ventilation started, backlayering diminishes and after 30 s LVS started, the velocity profiles show similar trend.

If Fig. 7 and Fig. 13 are analyzed together, it is seen that the smoke spreads faster for 50 MW fire case since the high HRR increases the backflow velocity. As seen in Fig.7 smoke reaches to entrance of tunnel in 30s before LVS started. For this reason, LVS should be started earlier as the HRR increases. So in the numerical

simulations for 50 MW fire, LVS were started after 10 seconds from the beginning of the fire.

A backflow velocity is seen at 6.8 m section while there is no backlayer at 2 m section, since smoke bubbles have not reached that section yet. The magnitude of the backflow velocity at 6.8m was approximately 0.9 m/s. After 30s from the start of LVS, the velocity profiles become similar to 30s of 10 MW fire.

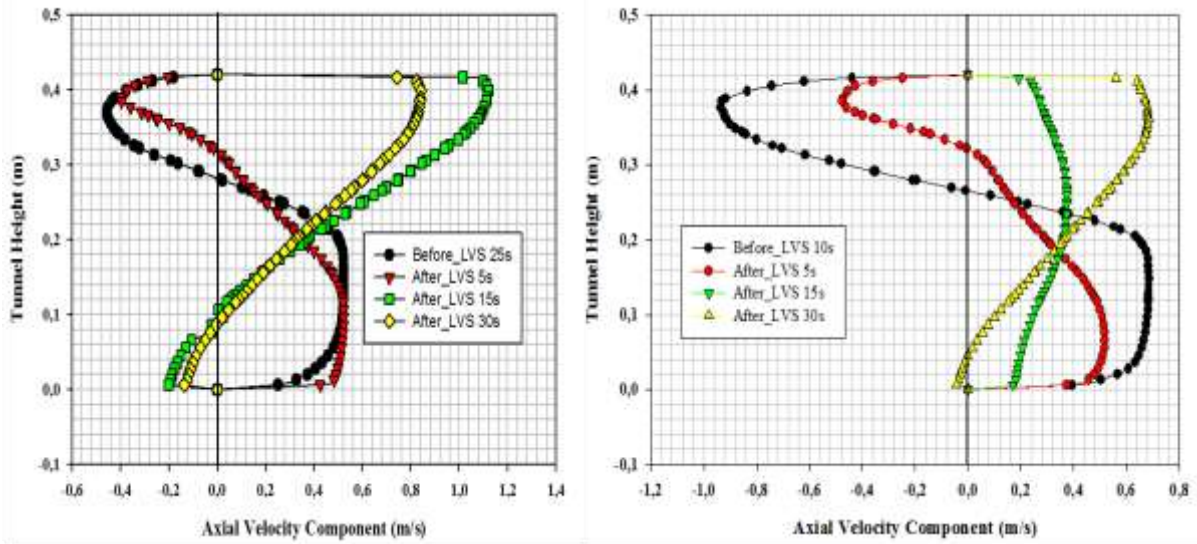


**Figure 10.** Axial velocity profiles on the vertical centreline of cross-section at 6 m from the tunnel entrance before and after LVS. (a) For 10MW fire case and (b) For 50 MW fire case.

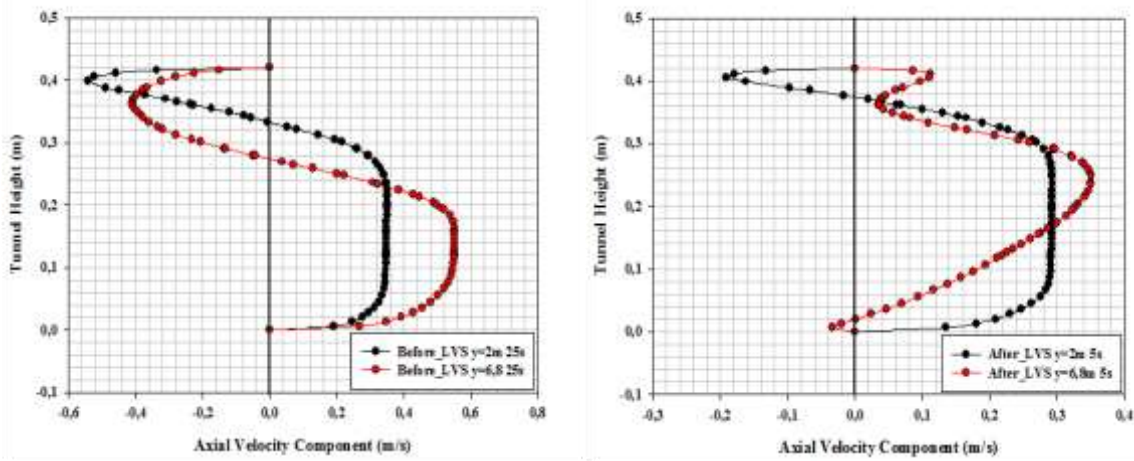


**Figure 11.** Axial velocity profiles on the vertical centreline of cross-section at 2m and 6.8 m from the tunnel entrance for cases 10MW (10FG1(2)+10FG2(1)).

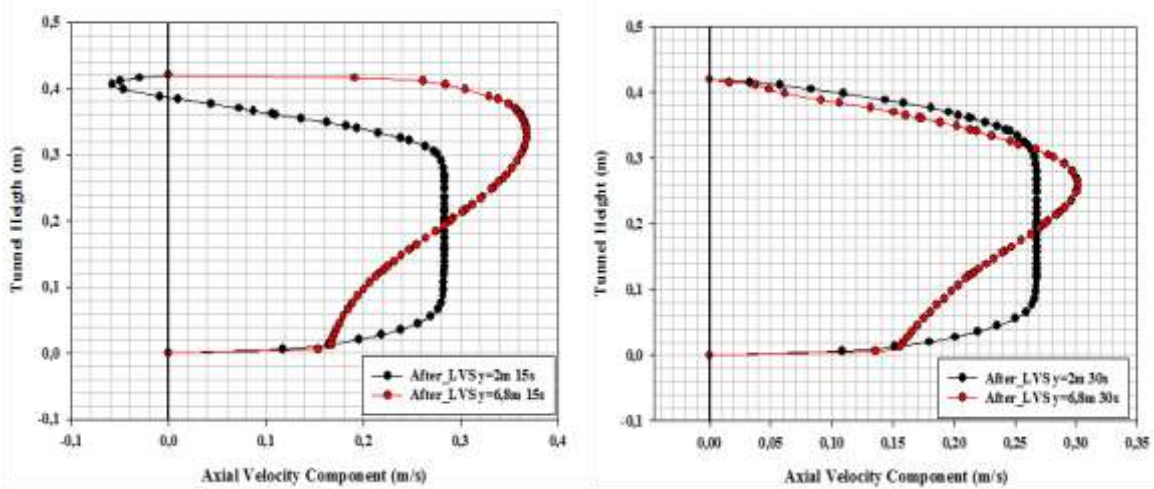


**Figure 12.** Axial velocity profiles on the vertical centreline of cross-section at 2m and 6.8 m from the tunnel entrance for cases 10MW (10FG1(2)+10FG2(1)).

In order to analyze smoke and air movement inside the tunnel, the streamline contours were drawn in suction of the fans. These negative velocities are also clearly seen in Fig. 10.

In order to analyze smoke and air movement inside the tunnel, the streamline contours were drawn in suction of

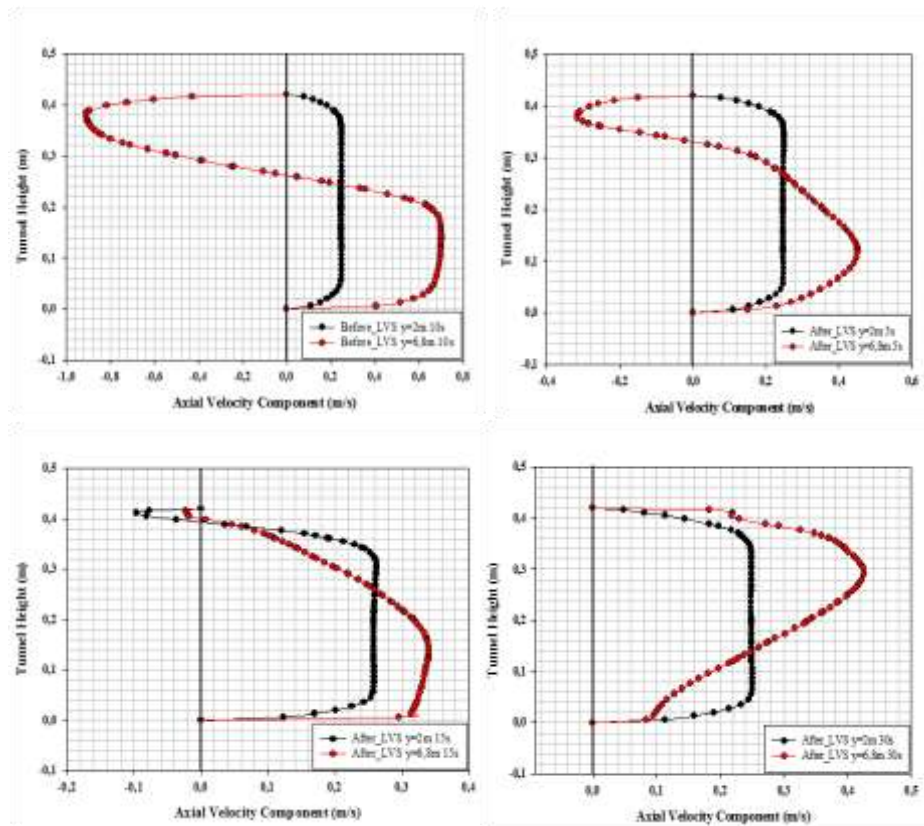


**Figure 13.** Velocity profiles on the centreline of cross-section pointed 2m and 6.8 m from the tunnel entrance for 50 MW (50FG1(2)).

the fans. These negative velocities are also clearly seen in Fig. 10.

Fig. 14. Negative velocities at the bottom part of the tunnel are seen below the fan groups due to Since the pressure jump in the fan group 1 is higher than the fan group 2, the circulation zone is much bigger below the fan group 1 near the bottom of the tunnel compared to the bottom region of the fan group 2.

The results of all simulation cases in Table 2 are not given in the manuscript, since those cases couldn't provide smoke discharge efficiently and couldn't decrease the temperature distribution satisfactorily in the tunnel. When those cases in Table 2 were analyzed, it is seen that, the case 10FG1(1) cleans the region behind the fan group 1, however it pushes the smoke only a few meters and so it is not able to clean the whole region between the fan group 1 and fan group 2. The case 50FG1 (1) is able to cease the smoke movement; however it could not able to prevent the spread of the smoke to the tunnel floor region, effectively. In order to see the effect of fan group 2 on fire smoke movement in the above cases, the fan group 2 is also operated with fan group 1. So the case, 50FG1 (1) + 50FG2 (1) in Table 2 is simulated numerically. The air velocity at the exit of these fans is very high and it helps efficiently to cool the fire, however it is not able to extract all of the smoke between fan groups. At the case 50FG1 (2) + 50FG2 (2), the velocity of the fan group 2 is faster compared to previous case and this

case is performed to see effects of suction of the fans on the fire. It cleans the region between the fans, however, the region below the fan group 2 and region near the fire pool, the smoke could not be removed completely due to the high velocities and turbulence near the fire pool. The case 50FG1 (2) + 50FG2 (1) is also considered. Decreasing pressure jumps of the jet fan group 2, the

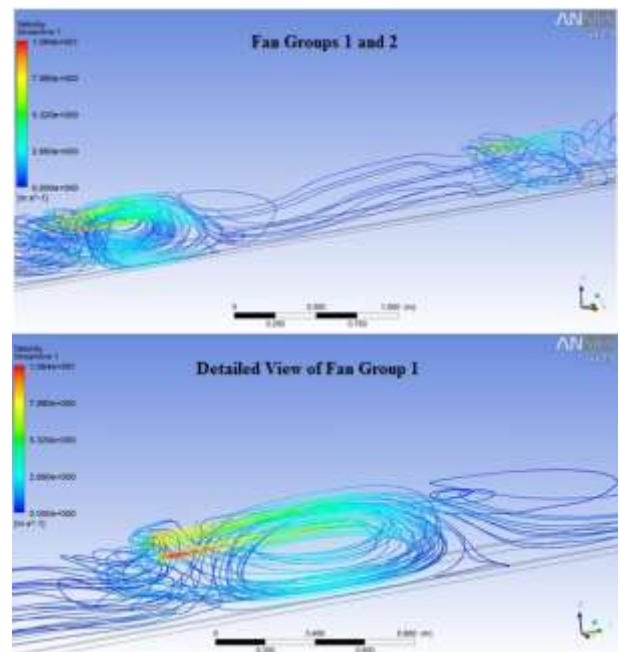


**Figure 14.** Streamline visualizations for jet fan group-1 at 10FG1(2)+10FG2(1) ventilation test code.

charge velocities seem to be more suitable to prevent backlayer, however there are some smoke bubbles in the tunnel floor. The smoke bubbles over the safety walkways cause difficulties in evacuation of people and fire extinction. The cases 50FG1(2)+ 50FG2(2)+ 50FG3(2) and 50FG1(2)+ 50FG2(1)+ 50FG3(2) are additional studies to see how the operation scheme of fan group 3 affect on extracting smoke. When all three groups of fans are operated at the same time, even though the fire gases get cold, the smoke spreads to the entire region between the fire pool and exit portal.

### Validation of the Numerical Results

The results of the simulations performed in this study were validated comparing them with results of the similar studies found in the literature. One validation was made by comparing the temperature distributions with the previous studies. The average temperature of fire ambient  $T_f$  obtained from the simulation results and calculated from the formula given in references ASHRAE Applications, Enclosed Vehicular Facilities (1999) and Li et al. (2003) were compared. For 10 MW fire case,  $T_f$  obtained from the simulated temperature contours shown in Fig. 15 was 380 K and  $T_f$  calculated as 370 K from the formula. In calculation of the ambient average temperature, the flame region temperature values were not taken into consideration due to high temperatures of the flame.

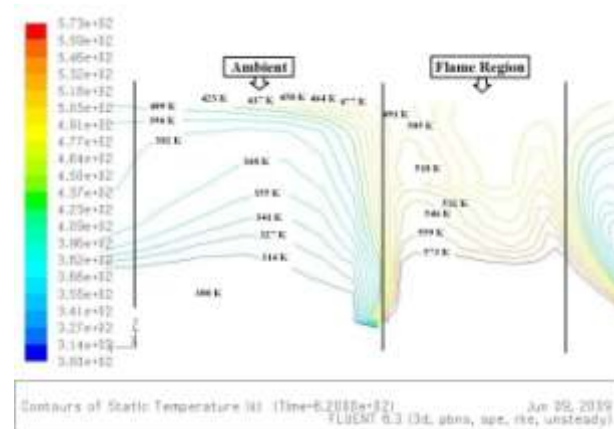


**Figure 15.** Temperature distributions at flame region and fire ambient for 10 MW fire case.

In Fig.8 and Fig.15, it is seen that the hot to cold region transition temperatures are 314 K and 332.5 K for 10 MW and 50 MW fire cases, respectively. It is known that the threshold temperature of human tolerance is 333 K. Hence, 50 MW fire may be dangerous and fatal for human.

Another data used for the validation of the model is Memorial Tunnel Case study Vega et al. (2008). This study is an important research that presents CFD results which are in good agreement with the experimental results. The cross-section used in that study is similar to the model of tunnel used in the present study. The transition temperature distributions of cold to hot zones

obtained in the present study are in quite agreement with the Memorial Tunnel Case study. Test cases of Vega et al. (2003) - (*Test606A and Test612B*) for 10 MW and 50 MW fires with different LVS applications, the transition temperature of cold to hot zone was measured as 70 °F (294 K) and 140 °F (333K) respectively. These transition temperatures are compatible with the results given in Fig. 7 and Fig. 8. Along longitudinal and vertical directions, there are some minor differences on smoke profiles. These differences may be due to the differences in the initial conditions, dimensions of the tunnels and the fire pool design. Barello et al. (2002) and McGrattan and Hamins (2002) studied LVS for tunnel fire with similar geometries. Temperature distributions of these studies are also in good agreement with our results.

An important point to be considered is that the air speed along the tunnel should not exceed 11 m/s. This velocity value is a limit to assure that people can escape from the tunnel (NEPA 2004). For our tunnel characteristics this velocity value scaled to 2.46 m/s. The axial velocity results show that the maximum axial velocity values for all ventilation strategy on the safety walkways are under this critical value.

### CONCLUSION

In this study, the different fire scenarios (10 MW and 50 MW fire cases), and the effect of LVS on the fire and smoke movement were numerically investigated by using commercial CFD code FLUENT. Transient simulations for turbulent flow with heat transfer were performed. The fire was simulated as multispecies mixture of gases with buoyancy effects. In the present study, the optimum ventilation scheme for human life and fire extinction for a short tunnel named *Asarkayası in Turkey* was investigated numerically.

From the simulations, it was observed that the smoke propagation was faster than the long tunnel studies found in the literature. It was also observed that the smoke velocity increases toward the tunnel entrance in the backlayer. In order to prevent this uncontrolled smoke movement, the best charge velocities and operation order of jet fan groups were determined numerically. Simulations showed that fans near the fire pool should not be operated or should be operated at low charge velocities. Operation of the fans located between the fire and the tunnel exit does not contribute to extraction of the smoke. Hence, it can be concluded that operation of the fans close to the fire pool and between the fire and tunnel exit causes the dispersion of smoke to clean regions.

The results obtained from the simulations showed how dangerous situations can appear in a short tunnel. But in reality, determination of the fire intensity, location etc. instantly is extremely difficult. However, today advanced measurement and control systems can be used, and in a reasonable time period, the characteristics

of the fire can be determined and the proper ventilation scheme can be utilized.

In summary, the results showed that CFD modelling gives satisfactory results on tunnel fires especially on the operation of LVS. Instead of expensive and complicated experiments, CFD simulations can be used as a powerful and reliable tool.

## REFERENCES

ASHRAE Applications, Enclosed Vehicular Facilities (1999), Chapter 12, 1791 Tullie Circle, GA 30329 N.E., Atlanta, USA.

Betta, V., Cascetta, F., Musto, M. and Rotondo, G., Numerical Study of The Optimization of The Pitch Angle of an Alternative Jet Fan in a Longitudinal Tunnel Ventilation System, *Tunnelling and underground Space Technology* 24(2), 164-172, 2009.

Betta, V., Cascetta, F., Musto, M. and Rotondo, G., Fluid dynamic performances of traditional and alternative jet fans in tunnel longitudinal ventilation systems, *Tunnelling and Underground Space Technology* 25, 415-422, 2010.

Borello, D., Giuli, G. and Rispoli, F., A CFD methodology for fire spread and radiative effects simulation in longitudinal ventilation tunnels: application to the memorial tunnel, *International PHOENICS User Conference 23-27 September- Moscow*, 2002.

Carvel, O. R., Fire Size in Tunnels, *PhD. Thesis, Heriot-Watt University School of the Built Environment Division of Civil Engineering Riccarton. Edinburgh: EH14 4AS*, 43-44, 2004.

EUREKA-Project EU 499: Firetun, *Fires in Transport Tunnels: Report on Full-Scale Tests*, Studiengesellschaft Stahlanwendung e.V., Düsseldorf 1995.

Hu, L. H., Huo, R., Wang, H. B., Li, Y. Z. and Yang, R. X., Experimental studies on fire-induced buoyant smoke temperature distribution along tunnel ceiling, *Building and Environment* 42, 3905-3915, 2007.

Hu, L. H., Huo, R. and Chow, W. K., Studies on buoyancy-driven back-layering flow in tunnel fires, *Experimental Thermal and Fluid Science* 32, 1468-1483, 2008.

Hu, L.H., Peng, W., Huo, R., Critical Wind Velocity for Arresting Upwind Gas and Smoke Dispersion Induced by Near- Wall Fire in Road Tunnel, *Journal of Hazardous Materials* 150, 68-75, 2008.

Hu, L. H., Tang, F., Yang, D., Liu, S. and Huo, R., Longitudinal distributions of CO concentration and difference with temperature field in a tunnel fire smoke flow, *International Journal of Heat and Mass Transfer* 53, 2844-2855, 2010.

Hwang, C.C. and Edwards, J.C., The critical ventilation velocity in tunnel fires—a computer simulation, *Fire Safety Journal* 40, 213-244, 2005.

Jojo S.M.L. and Chow, W.K., Numerical studies on performance evaluation of tunnel ventilation safety systems, *Tunnelling and Underground Space Technology* 18, 435-452, (2003).

Kurioka, H., Oka, Y., Satoh, H. and Sugawa, O., Fire properties in near field of square fire source with longitudinal ventilation in tunnels, *Fire Safety Journal* 38, 319-340, 2003.

Lee, S. R. and Ryou, H. S., A numerical study on smoke movement in longitudinal ventilation tunnel fires for different aspect ratio, *Building and Environment* 41, 719-725, 2006.

McGrattan, K. B. and Hamins, A., Numerical Simulation of the Howard Street Tunnel Fire, Baltimore, Maryland Building and Fire Research Laboratory, *National Institute of Standards and Technology (NISTIR 6902)*, 12, 2002.

Modic, J., Fire simulation in road tunnels, *Tunnelling and underground Space Technology* 18, 525-530, 2003. National Fire Protection Association, "NFPA 502 Standard for Road Tunnels, Bridges, and Other Limited Access Highways 2004 Edition" 2004, National Fire Protection Association, 1 Batterymarch Park, Quincy, MA 02169-7471.

PIARC, Committee on Road Tunnels, 1999. Fire and Smoke Control in Road Tunnels.

Tajadura, R. B., Morros, C. S. and Marigorta, E.B., Influence of The Slope in The Ventilation Semi-Transversal System of an Urban Tunnel, *Tunnelling and underground Space Technology* 21, 21-28, 2006.

Vauquelin, O., Wu, O. and Wu, Y., Influence of Tunnel Width on Longitudinal Smoke Control, *Fire Safety Journal* 41, 420-426, 2006.

Vega, M. G., Diaz, K. M. A., Oro, J. M. F., Tajadura, R. B. and Morros, C. S., Numerical 3D simulation of a longitudinal ventilation system: Memorial Tunnel Case, *Tunnelling and underground Space Technology* 23, 539-551, 2008.

Wu, Y. and Bakar, M. Z. A., Control of smoke flow in tunnel fires using longitudinal ventilation systems—a study of the critical velocity, *Fire Safety Journal* 35(4), 363-90, 2000.



**Salih KARAASLAN** was born in Ankara in 1981. He was graduated from Gazi University, Mechanical Engineering Department in 2003, in Turkey. After graduation he worked as a R&D engineer in Hidrosan Damper Industry for a year. He received his M.Sc. degree from Institute of Natural and Applied Science of Gazi University in Turkey, in 2006. He has been working as a research assistant since 2004 at Gazi University Mechanical Engineering Department. He is still working on his Ph.D studies. His major interest of study is numerical and experimental combustion, tunnel fire and ventilation systems, energy systems and internal combustion engines.



**Ender HEPKAYA** was born in Samsun in 1987. He was graduated from Gazi University, Mechanical Engineering Department in 2009, in Turkey. He received his M.Sc. degree from Institute of Natural and Applied Science of Gazi University in Turkey, in 2013. He joined in TUSAŞ Engine Industry in 2013. His major interest of study is numerical and experimental combustion, gas turbines, tunnel fire and ventilation systems, and internal combustion engines.



**Nuri YUCEL** was graduated from Istanbul Technical University, Mechanical Engineering Department in 1979, in Turkey. After graduation he worked as a maintenance engineer in Turkish Petroleum Corporation for 2 and half year. He received his M.Sc. degree from Polytechnic Institute of New York in U.S.A, in 1984, and Ph.D. degree in Polytechnic University of New York in U.S.A, in 1988. Yucel is a member of Turkish Chamber of Mechanical Engineers and Turkish Society for Thermal Science and Technology. He is the editor-in-chief of Journal of Thermal Science and Technology. His major interest of study is numerical and experimental heat transfer, fluid flow, energy systems and internal combustion engines. He worked as an assistant professor between 1988 and 1991 at Anadolu University in Eskisehir, Turkey. Later, he joined in Gazi University. He has been working as a full professor since 2000. He has many conference and journal papers.